Brain activations time locked to slow wave-coupled sleep spindles correlates with intellectual abilities

Baena, Daniel,[a] Fang, Zhuo,[b] Ray, Laura B.,[b] Owen, Adrian M., [d,e] & Fogel, Stuart M.[a,b,c,d]

[a]Sleep Unit, University of Ottawa Institute of Mental Health Research at The Royal, Ottawa, Canada
[b]School of Psychology, University of Ottawa, Ottawa, Canada
[c]University of Ottawa Brain & Mind Research Institute, Ottawa, Canada
[d]The Brain & Mind Institute, Western University, London, Canada
[e]Department of Physiology and Pharmacology and Department of Psychology, Western University, London, Canada

Corresponding Author:
Dr. Stuart M. Fogel
Associate Professor
School of Psychology
University of Ottawa
Ottawa, Ontario K1N 6N5
sfogel@uottawa.ca

Abstract

Sleep spindles (SP) are one of the few known electrophysiological neuronal biomarkers of interindividual differences in cognitive abilities and aptitudes. Recent simultaneous EEG-fMRI studies suggest that the magnitude of the activation of brain regions recruited during spontaneous spindle events is specifically related to Reasoning abilities. However, it is not known if the relationship with cognitive abilities differs between uncoupled spindles, uncoupled slow waves (SW) and coupled SW-SP complexes, nor have the functional neuroanatomical substrates that support this relationship been identified. Here we investigated the functional significance of activation of brain areas recruited during SW-coupled spindles, uncoupled spindles, and uncoupled slow waves. We hypothesize that brain activations time locked to SW-coupled spindle complexes will be primarily associated to Reasoning abilities, especially in subcortical areas. Our results provide direct evidence that the relationship between Reasoning abilities and sleep spindles depends on spindle coupling status. Specifically, we found that the putamen and thalamus, recruited during coupled SW-SP events were positively correlated with Reasoning abilities. In addition, we found a negative association between Reasoning abilities and hippocampal activation time-locked to uncoupled SWs that might reflect a refractory mechanism in the absence of new, intensive hippocampal-dependent memory processing.

Keywords: sleep, spindles, cognitive abilities, simultaneous EEG-fMRI, NREM

Introduction

The microarchitectural features of sleep are some of the few known electrophysiological neuronal biomarkers of interindividual differences in cognitive abilities (Schabus et al. 2006; Ujma et al. 2015; Fang et al. 2017). Sleep spindles were the first sleep feature to be identified (for review, see: (Fogel and Smith 2011), and continue to be the focus of ongoing investigations, primarily in an effort to better understand the specificity of this relationship, and associated the neural correlates/substrates. The characteristics of spindles are trait-like; they are consistent from night-to-night within an individual, yet they differ greatly between individuals (Silverstein and Levy 1976; Gaillard and Blois 1981; de Gennaro et al. 2005). Spindles have been referred to as an "*electrophysiological fingerprint*", yet, the functional significance of this unique signature remains to be fully understood. It is clear however, from over 20 years of the most recent research on the spindle, that they are critically important for memory processing and intimately related to intellectual function. The interindividual differences in spindle characteristics have been found to be related to the capacity for reasoning. Reasoning involves cognitive abilities required identify complex patterns and relationships, the use of logic, planning and skills that are required to solve novel problems (Bódizs et al. 2005; Schabus et al. 2006; Fogel et al. 2007; Bódizs et al. 2008; Nader and Smith 2009; Fang et al. 2017). Reasoning abilities are analogous to cognitive abilities that support *"fluid intelligence"* (Cattell 1963). See methods for a detailed description of Reasoning abilities and the testing approach. Furthermore, when accounting for the overlap between

various cognitive subdomains (Fogel et al. 2007; Fang et al. 2017), spindle characteristics are not associated with verbal cognitive abilities, *i.e.*, "*crystalized intelligence*", which reflect the ability to use and remember facts, figures, events, places, *etc*. Thus, supporting the idea that spindles are an electrophysiological biomarker of specific individual differences in cognitive strengths and weaknesses; particularly for the capacity to solve problems through logic and reasoning.

The brain areas recruited during spontaneous spindle events have been identified using simultaneous EEG and fMRI. These areas include the thalamus and the temporal lobe (Laufs et al. 2007; Schabus et al. 2007; Tyvaert et al. 2008; Andrade et al. 2011; Caporro et al. 2012), as well as activation of the cingulate cortex and motor areas (Andrade et al. 2011; Caporro et al. 2012). Interestingly, activation of areas related to memory and cognitive function like the putamen (Tyvaert et al. 2008; Caporro et al. 2012), basal ganglia (Tyvaert et al. 2008; Caporro et al. 2012; S.M. Fogel et al. 2017) and hippocampus (Schabus et al. 2007) are also activated time-locked to spindle events.

However, spindles do not always occur in isolation. Rather, they are often part of *slow wave – spindle – hippocampal ripple* complexes, whereby ripples are nested in the excitatory troughs of spindles, and spindles are nested in the excitatory troughs ("up-states") of slow waves (Helfrich et al. 2019). Slow wave – spindle (SW-SP) coupling is associated with memory consolidation both in young and older adults and is considered an index of neural plasticity (Maingret et al. 2016; Bergmann and Born 2018; Helfrich et al. 2018; Ngo et al. 2020). Recent results from our group have identified

dissociable patterns of brain activation when comparing slow wave-coupled spindles, uncoupled spindles, and, uncoupled slow waves (Baena et al. 2022). Critically, activation of the putamen was observed only during slow wave-coupled spindles, and recruitment of the hippocampus was observed only during isolated slow waves and coupled spindles, but not during isolated spindles. Thus, suggesting that spindles may not be the only electrophysiological index of cognitive abilities. However, this possibility remains to be directly investigated, and is the main aim of the current study.

Recent simultaneous EEG-fMRI studies aimed to assess the relationship between brain activity time locked to spindle events and cognitive abilities. A recent study by our group (Fang et al. 2019) investigated the relationship between brain activity time-locked to spindle events and interindividual differences in cognitive abilities for Short-Term Memory, verbal intelligence, and fluid intelligence. Remarkably, only fluid intelligence was associated with cerebral activations occurring during spindles events. Specifically, brain activation of the thalamus, prefrontal cortex (PFC), putamen, cerebellum and the precuneus was associated with fluid intelligence, but not verbal intelligence or Short-Term Memory abilities. In addition, the strength of functional connectivity within the cortical-striatal and thalamo-cortical networks was associated with fluid intelligence, but not with verbal intelligence or Short-Term Memory abilities (Fang et al. 2020). Taken together, these findings suggest that spindles are not only uniquely related to fluid intelligence, but also, that the magnitude of the activation of brain regions recruited during spontaneous spindle events, and the strength of the related functional communication between regions

92 is specifically related to fluid intelligence. Thus, spindles are a physiological index of fluid intelligence,
93 and an electrophysiological marker of the functional-neuroanatomical substrates which support
94 intellectual function.

95 We have recently identified unique functional brain activations that are specific to SW-SP
96 complexes (Baena et al. 2022). Trait-like aspects of spindles are considered biological markers of
97 interindividual differences in intellectual abilities. However, we did not previously explore how brain
98 activations associated with SW-SP coupling relates to intellectual abilities. Thus, the functional
99 significance of activations time-locked to coupled SW-spindle complexes in comparison to activations
100 specific to uncoupled spindles and uncoupled slow waves remains to be explored. In line with previous
101 studies, we expect to observe a relationship between spindles and Reasoning abilities (*i.e.*, fluid
102 intelligence). We hypothesize that brain activations time locked to SW-coupled spindle complexes will
103 be primarily associated to fluid intelligence, especially in subcortical areas important for planning,
104 problem-solving, reasoning, and strategy such as the striatum, hippocampus and the frontal lobe, as
105 well as areas important for spindle generation, such as the thalamus.

106 ## Methods

107 ### Participants

108 All participants were initially screened for irregular sleep schedules (bedtime outside the hours of
109 ~22:00-24:00 h, wake time outside the hours of 07:00-09:00 h), left-handedness, shift work, and the use

of medications known to affect sleep. Participants were also not eligible to participate if they considered themselves a smoker, consumed >1-2 caffeinated beverages/day, consumed >7 alcoholic beverages/week, or had a history of chronic pain, seizures or head injury. Participants completed the Beck Depression (Beck, Steer, et al. 1988) and Anxiety Inventories (Beck, Epstein, et al. 1988) as well as the Sleep Disorders Questionnaire (Douglass et al. 1994) to exclude participants with signs of depression or anxiety and ensure normal sleep-wake patterns. Three days prior to, and throughout participation in the study, participants were required to refrain from recreational drug use and limit caffeine (to no more than 1 beverage in the AM) and alcohol intake. Actigraphy and sleep logs were used to confirm the participants' sleep and activity cycles throughout the study. A total of 35 participants were recruited, seven participants did not meet study inclusion criteria. In total, N = 28 participants (mean age 24, 16 females) were included in the final data analyses.

Ethics statement

All study procedures and methods adhered to the Declaration of Helsinki and were approved by the Western University Health Science research ethics board. All participants were given a letter with details of the study, provided informed consent, and were financially compensated for their participation.

Procedures

All participants who met the study inclusion criteria underwent an orientation session where they were given the study instructions, detailed instructions of the online Cambridge Brain Sciences (CBS)

tests (see below), a sleep diary and an activity monitor to verify their sleep–wake cycle (**Figure 1**). After the orientation session, all participants were required to complete the CBS test battery (Hampshire et al. 2012). It takes around 30-45 minutes to complete the CBS tests. A minimum of one week following the orientation session, participants completed the EEG-fMRI sleep recording night. Participants arrived at the sleep laboratory on the recording night at approximately 20:00 h. EEG equipment was installed and configured prior to scanning procedures beginning at 21:00 h. Localizer scans, a T1 structural scan, and an 8-minute eyes-closed awake resting-state scan were completed. To confirm that participants remained awake in the MRI scanner prior to the sleep session, EEG was acquired during the initial scanning procedures. The EEG-fMRI sleep session began at about 22:00 h, within the range of the participants' habitual bedtime, and ended no later than midnight (24:00 h), or if participants terminated the session early, e.g., due to inability to sleep or discomfort. Participants slept the rest of the night in the nearby sleep laboratory after the EEG-fMRI sleep session. Only the sleep EEG acquired in the scanner was used in the data analysis.

Figure 1 insert

Intelligence testing

The CBS platform is a web-based test battery, which has previously been used in both large-scale population-sized (Hampshire et al. 2012; Wild et al. 2018) and smaller-scale studies (Fang et al.

2017; Laventure et al. 2018; Brewer-Deluce et al.). CBS tests have a number of advantages over other tests of cognition, including ease of administration and the fact that the neural correlates of each subtest have been investigated using functional neuroimaging (Hampshire et al. 2012). The CBS trials includes 12 cognitive tests that measure a broad range of cognitive abilities including reasoning, problem solving, planning, attention, and memory. CBS trials are adapted from well-known, well-established paradigms from the cognitive neuroscience literature that test a wide range of aspects of cognition. CBS subscales (*i.e.*, Verbal, Reasoning and Short-Term Memory) are derived quantitatively from a data-driven approach using factor analysis, conducted on a large population (>44,000 individuals) from a previous study (Hampshire et al. 2012) in contrast to conventional tests which are based solely on the face-validity of the constructs of interest. The Reasoning factor is best described in terms of performance on five classical tests adapted for online testing from the cognitive and neuropsychological literature, including deductive reasoning (Cattell 1940), spatial rotation (Silverman et al. 2000), feature match (Treisman and Gelade 1980), spatial planning (Shallice 1982), and polygons (Folstein et al. 1975). STM is best described in terms of four tests, including visuospatial working memory (Inoue and Matsuzawa 2007), spatial span (Corsi 1973), paired associates (Gould et al. 2006), and self-ordered search (Collins et al. 1998). Finally, verbal ability is best captured by performance on three tests, including verbal reasoning (Baddeley 1968), color-word remapping (Stroop 1935), and digit span (Wechsler 1981). Raw scores from each of the 12 subtests were normalized using the mean and standard deviation obtained

from a large, young population (N = 44,600; age 20–35 years) of participants who completed the CBS Trials (Hampshire et al. 2012). Each subtest was then weighted according to the factor loadings from Hampshire et al. (2012). Finally, the respective sub-tests were averaged to create the Reasoning, STM, and Verbal sub-scales and transformed to standard scores. Importantly, and particularly for the aims of the current study, sleep spindles have been found to be correlated specifically with Reasoning ability scores derived from the CBS test battery, using the same testing approach used here (Fang et al. 2017). In addition, the neural correlates of each factor have been investigated previously using neuroimaging (Hampshire et al. 2012), and have been shown to depend on distinct neural correlates. Thus, we chose the CBS platform to investigate the neural correlates between sleep spindles and cognitive abilities.

CBS Score Calculation

Raw scores from each of the 12 subtests were normalized using the mean and standard deviation obtained from a large, young population (N = 44,600; age 20–35 years) of participants who completed the CBS Trials (Hampshire et al. 2012). Each subtest was then weighted according to the factor loadings from Hampshire et al. (2012). Finally, the respective sub-tests were averaged to create the Reasoning, STM, and Verbal sub-scales and transformed to standard scores, so that test scores were readily comparable to results from similar studies that employed test batteries tapping into Reasoning and Verbal abilities, such as the Multidimensional Aptitude Battery – II (Fogel and Smith 2006; Fogel et al. 2007) and other commonly used batteries of cognitive abilities such as the Wechsler

181 Adult Intelligence Scale (Wechsler 1981). The descriptive statistics of each subtest are shown in **Table**
182 **1**.

183 **Table 1**.

184

185

186 **Polysomnographic Acquisition and Analysis**

187 ***Polysomnographic Recording Parameters.*** Polysomnographic (PSG) recordings were obtained using a
188 64-channel magnetic resonance (MR)-compatible EEG cap, which included one electrocardiogram
189 (ECG) lead (Braincap MR, Easycap) and 64-channels of EEG recorded via two MR-compatible 32-
190 channel amplifiers (Brainamp MR Plus, Brain Products GmbH). EEG recordings were referenced to FCz
191 and digitized at 5000 samples per second with a 500-nV resolution. Three additional bipolar ECG
192 recordings were taken using a MR-compatible amplifier (Brainamp ExG MR, Brain Products GmbH) to
193 account for the limited visualization of the r-peak of the QRS complex when using a single ECG lead
194 included in the EEG cap. In order to reduce ballistocardiographic (BCG) artifacts by up to 40% (Mullinger
195 et al. 2011), participants were positioned in the MRI scanner so that they were shifted away from the
196 isocenter of the magnetic field by 40 mm, making BCG correction more straightforward. Data were
197 analog filtered using a 500 Hz band-limiter low-pass filter and a 0.0159 Hz high-pass filter with a 10-sec

198 time constant. Data was recorded with Brain Products Recorder Software, Version 1.x and transferred
199 to the recording computer via fiber-optic cable and hardware synchronized to the scanner clock using
200 the Brain Products “Sync Box” (Brain Products GmbH). As recommended in the literature (Mulert and
201 Lemieux 2010), the MRI sequence parameters were selected to ensure that the gradient artifact would
202 be time stable, and that the lowest harmonic of the gradient artifact (18.52 Hz) would occur at the highest
203 possible frequency and above the spindle band (11–16 Hz). Thus, the MR scan repetition time was set
204 to 2160 msec, matching a common multiple of the EEG sample time (0.2 msec), the product of the
205 scanner clock precision (0.1 μsec), and the number of slices (40) used.

206 ***EEG Preprocessing.*** EEG scanner artifacts were removed in several steps. First, an adaptative
207 average template subtraction method (Allen et al. 2000) implemented in Brain Products Analyzer
208 Software, Version 2.x was used and data was downsampled to 250 Hz. Next, r-peaks in the ECG were
209 detected semi-automatically. Each r-peak was visually verified and, when necessary, manually adjusted
210 to correct both false-positive and false-negative r-peak detections, to ensure an optimal BCG correction.
211 Next, adaptive template subtraction (Allen et al. 1998) was used to remove BCG artifacts time-locked
212 to the r-peak of the QRS complex. After MRI-related artifact correction, data was visually inspected and
213 amplitude of the residual artifacts time-locked to the r-peaks were examined. An independent
214 component-analysis-based approach (Srivastava et al. 2005; Mantini et al. 2007) was applied to remove
215 any remaining BCG residual artifacts if the peak of the maximum amplitude of the residual artifact

exceeded 3 μV during the QRS complex (*e.g.*, 0–600 msec). Lastly, the EEG was re-referenced to the averaged mastoids and a low-pass filter of 60 Hz was applied. Following preprocessing, sleep stages were scored in accordance with standard criteria (Iber et al. 2007) using the "VisEd Marks" toolbox (https://github.com/jadesjardins/vised_marks) for EEGLAB (Delorme and Makeig 2004).

Slow Wave Detection. Slow waves were automatically detected from Fz, Cz and Pz during movement artifact-free NREM sleep (N2 and SWS) via a period amplitude analysis detection algorithm (https://github.com/stuartfogel/Period-Amplitude-Analysis) based on methods previously described (Bersagliere and Achermann 2010), adapted for EEGlab (Delorme and Makeig 2004) and written for MATLAB R2019b (The MathWorks Inc.). First, the EEG signal was band-pass filtered (32nd order Chebyshev Type 2 low-pass filter, 80 dB stopband attenuation, 2.15 Hz frequency cut-off; 64th-order Chebyshev type 2 high-pass filter, 80 dB stopband attenuation, 0.46 Hz frequency cut-off). The cut-off frequencies were selected to achieve minimal attenuation in the band of interest while keeping a good attenuation of the neighboring frequencies. The filters were applied in the forward and reverse directions to achieve zero-phase distortion. Next, half-waves were determined as negative or positive deflections between two consecutive zero crossings in the band-pass filtered signal for frequencies between 0.5 and 2 Hz. Only adjacent half-waves with a peak-to-peak amplitude higher than 75 μV and longer than 0.25 seconds were considered for the analysis. The latency of the negative peak of each slow wave was extracted for further analyses.

234 ***Spindle Detection.*** Sleep spindles were automatically detected from Fz, Cz, and Pz during
235 movement artifact-free NREM sleep (N2 and SWS) using an established (Fogel et al. 2014; Albouy et
236 al. 2015; Fang et al. 2017; Fang et al. 2019) and validated (Ray et al. 2015) method employing EEGlab-
237 compatible (Delorme and Makeig 2004) software (https://github.com/stuartfogel/detect_spindles) written
238 for MATLAB R2019b (The MathWorks Inc.). Detailed processing steps, procedures, and method
239 validation are reported elsewhere (Ray et al. 2015). Briefly, the spindle data were extracted from
240 movement artifact-free, NREM epochs. The detection method (Ray et al. 2015) used a complex
241 demodulation transformation of the EEG signal with a bandwidth of 5 Hz centered about a carrier
242 frequency of 13.5 Hz (*i.e.*, 11–16 Hz). The method employs an adaptive amplitude threshold at the 99th
243 percentile on the transformed signal. Spindles were visually verified by a single expert scorer after
244 automatic detection. The variables of interest extracted from this method include spindle amplitude,
245 duration, and density (number of spindles/minute of NREM sleep) for each participant. From the spindle
246 data, the onset and peak of each spindle event was extracted for further analyses.

247 ***Slow Wave-Spindle Coupling.*** Using the slow wave negative peak latencies and the spindle peak
248 latencies from Fz, Cz, and Pz, we performed coupling detection procedures using the approach
249 developed by Mölle and colleagues (Mölle et al. 2011) employing EEGlab-compatible (Delorme and
250 Makeig 2004) software written for MATLAB R2019b (The MathWorks Inc.). The spindles were then
251 marked as coupled SW-SP complexes when the spindle peak onset occurred within a 4-second time

252 window built around the slow wave negative peak. Due to the low number of coupled spindle events on
253 each individual channel, detections from Fz, Cz and Pz were used in the final analyses. In the same
254 way, it was not possible to further subdivide events into slow and fast spindle categories. Lag was
255 measured as the distance between the slow wave negative peak and the spindle peak latency. Coupling
256 strength was measured as the lag variance for each participant. Paired sampled t-tests were used for
257 the comparison of the SW-SP complexes, measured in time bins of 200ms along the 4 s window.
258 Percentage of coupled spindles relative to total number of spindles was calculated alongside the
259 percentage of coupled spindles relative to the total number of slow waves detected.

260 Additionally, the phase of the bandpass-filtered slow-wave signal in radians at the spindle onset
261 location was computed. The mean direction of the phase angles for all coupled spindle events were
262 determined using the CircStat toolbox (Berens 2009). Preferred phase of SW-SP coupling for each
263 participant was computed by averaging all individual event preferred phases. Finally, we performed
264 uniformity tests (Rayleigh test) and uniformity using positive slow wave peaks as the predefined mean
265 direction (V-test).

266 **Relationship Between Sleep Spindle EEG Characteristics and Cognitive Abilities**

267 Linear regression analyses were used to examine the effects of sleep spindles on cognitive
268 abilities (Reasoning, STM, and Verbal) assessed by the CBS test battery. Sleep spindle duration,
269 amplitude, and density were entered into each model as independent variables together; Reasoning,

STM, and Verbal subscale factors were entered into the models as dependent variables separately. Given that the relationship between spindles and Reasoning ability was reportedly different in men and women (Ujma et al. 2014), and brain volume might influence NREM slow wave oscillations (Saletin et al. 2013), sleep quality (Branger et al. 2016), or be related to cognitive abilities (Casey et al. 2005), regression models included gender and whole brain volume as covariates of non-interest.

MRI Acquisition and Analysis

MRI Recording Parameters. Images were obtained using a 3.0 Tesla Magnetom Prisma MRI system (Siemens) with a 64-channel head coil. Structural T1-weighted MRI images were acquired using a 3-D MPRAGE sequence (repetition time [TR] = 2300msec, echo time = 2.98 msec, inversion time = 900 msec, flip angle = 9°, 176 slices, field of view = 256 × 256 mm^2, matrix size = 256 × 256 × 176, voxel size = 1 × 1 × 1 mm3). During the sleep session, multislice T2*-weighted fMRI images were acquired using an EPI sequence using axial slice orientation (TR = 2160 msec, echo time = 30 msec, flip angle = 90°, 40 transverse slices, 3-mm slice thickness, 10% interslice gap, field of view = 220 × 220 mm^2, matrix size = 64 × 64 × 40, voxel size = 3.44 × 3.44 × 3 mm^3). Up to 2 hours of sleep EEG-fMRI data was acquired among all participants during fMRI acquisition.

Image Preprocessing. Functional images were preprocessed and analyzed using SPM12 (www.fil.ion.ucl.ac.uk/spm/software/spm12/; Welcome Department of Imaging Neuroscience) implemented in MATLAB R2015a (The Mathworks Inc.). fMRI images were corrected for slice

288 acquisition time differences and realigned to correct head motion using rigid body transformation. A
289 mean realigned image was then created from the resulting images. The structural T1 image was
290 coregistered to this mean functional image using a rigid body transformation optimized to maximize the
291 normalized mutual information between the two images. Coregistration parameters were then applied
292 to the realigned BOLD time series. The coregistered structural images were segmented into gray matter,
293 white matter, and cerebrospinal fluid. An average participant-based template was created using
294 DARTEL in SPM12. All functional and anatomical images were spatially normalized using the resulting
295 template, which was generated from the structural scans. Finally, spatial smoothing was applied on all
296 functional images (Gaussian kernel, 8-mm FWHM).

297 ***First-Level (within-subject) GLM.*** The onset and duration for each coupled SW-SP, uncoupled
298 spindles and slow wave event were identified from the EEG data and considered events of interest.
299 Friston-24 movement parameters (Friston et al. 1996), the mean white matter intensity, and the mean
300 cerebral spinal fluid intensity for each participant were entered into the model as nuisance variables. To
301 remove low frequency drifts from the time series, a high-pass filter with a cut-off at 128 seconds was
302 used. Brain activations time-locked to each event type (*e.g.*, spindle, SW and coupled SW-SP events)
303 were estimated using the onset and duration of each event in a fixed-effects GLM using an event-related
304 fMRI design. The BOLD time series data were modeled using the canonical hemodynamic response
305 function (HRF). The temporal and dispersion basis function derivatives were also included in the model

306 to account for the variability in the latency of the peak response and variability in the duration of the
307 peak response. Consequently, this approach yields an "*informed basis set*", generating three contrast t-
308 maps, one for the canonical HRF, one for the temporal derivative, and one for the dispersion derivative,
309 for each participant.

310 **ROIs selection**

311 Based on the spindle-related brain activation results consistently found in previous studies and
312 to directly address the main aims of the current study, seven pre-defined anatomical ROIs were selected
313 from the previous literature (Schabus et al. 2007; Tyvaert et al. 2008; Andrade et al. 2011; Caporro et
314 al. 2012; Sandman et al. 2014; S. Fogel et al. 2017; Fang et al. 2020; Fang et al. 2021; Baena et al.
315 2022), and built using WFUpickatlas AAL template including bilateral putamen, bilateral thalamus,
316 bilateral hippocampus, anterior cingulate cortex (ACC), middle cingulate cortex (MCC), superior
317 prefontal cortex (SPFC), and middle frontal gyrus (MFG). In addition, it should be noted that activation
318 of the thalamus, ACC, MCC and bilateral putamen during spindle events have been found to be
319 correlated specifically with Reasoning abilities (Fang et al. 2019; Fang et al. 2020).

320 **Regression analyses**

321 The activation beta values in the selected ROIs were extracted for coupled spindle (SW-SP),
322 uncoupled spindle, and uncoupled slow wave contrast maps respectively using Marsbar. Next, linear
323 regression analyses were conducted to explore the relationship between CBS tests scores (*i.e.*,

Reasoning, Verbal, STM) and the brain activation for each event type (*i.e.*, coupled SW-SP events, uncoupled spindles, uncoupled slow waves) respectively in SPSS version 24.0 (IBM Corp., 2016). The brain activation in the pre-defined ROIs was included in the model as the dependent variable. Scores of the three subtests were included together in the regression model as independent variables, with the whole brain gray matter volume as the covariate of no interest. Finally, follow-up direct comparisons between significant partial correlation coefficients were performed between coupled SW-SP events and uncoupled events using the toolbox by Lenhard & Lenhard (Lenhard and Lenhard 2014).

Results

Sleep architecture

All participants had more than 14 minutes of sleep during the EEG-fMRI recording session, and on average, there was 45 minutes (*SD* = 24) of sleep in total. Average sleep latency was 7.71 minutes (*SD* = 10), and the average time when participants fell asleep in the scanner was at 22:22h (*SD* = 26). NREM sleep data from 28 participants were included in the analyses. The average duration of NREM sleep included in the analyses was 40 minutes (*SD* = 19 minutes). Sleep architecture for the sample is summarized in **Table 2**.

Table 2

EEG characteristics of coupled SW-SP and uncoupled spindles

342 On average, 215 coupled spindles and 264 uncoupled spindles per participant were identified
343 and were included in the analyses. Detailed characteristics of the coupled SW-SP and uncoupled
344 spindles are summarized in **Table 3**. No differences between coupled SW-SP and uncoupled spindles
345 in terms of the number ($t(27) = -0.56$, $p = 0.58$) duration ($t(27) = -0.16$, $p = 0.87$) or density ($t(27) = -0.66$,
346 $p = 0.51$), were observed. Thus, suggesting an even distribution for each event type. Spindle amplitude
347 was significantly higher in coupled SW-SP in comparison to uncoupled spindles ($t(27) = 3.61$, $p = 0.001$),
348 suggesting that the characteristics of coupled spindles are significantly different from isolated spindles.

349 **Table 3**

350

351 Inspection of the temporal distribution of spindles co-occurring within the 4 sec window around
352 the negative peak of the slow wave (**Figure 2A**) revealed that the percentage of coupled spindles during
353 the up-to-down state ranging from -1 to 0 sec was significantly higher than the preceding interval ranging
354 form -2 to -1 sec ($t(27) = -5.41$, $p < 0.001$). Likewise, the percentage of coupled spindles during the
355 down-to-up state ranging from 0 to 1 sec), was also higher than the succeeding 1 to 2 sec interval ($t(27)$
356 $= 5.83$, $p < 0.001$). Finally, the percentage of coupled spindles during the down-to-up state was
357 significantly higher than during the up-to-down state ($t(27) = -3.05$, $p = 0.005$).
358 Next, to investigate the phase relationship between spindles and slow waves, the slow wave
359 phase at the spindle maximum for each SW-SP event was extracted and mean phase angle per

individual was computed (**Figure 2B**). Coupling of spindle events within the slow wave cycle was maximal, shortly before the down-to-up state peak in 15 out of 28 participants (0^{o}; $p < 0.001$, V-test). Further individual-level analyses revealed a non-uniform distribution ($p < 0.05$, Rayleigh test) of the preferred phases of SW-SP in 12 out of 28 participants, suggesting that spindles were coupled to slow waves preferentially adjacent to, or immediately following the positive slow wave peak, during the down-to-up state.

Figure 2 insert

Relationship between coupled and uncoupled spindle EEG characteristics and cognitive abilities

Consistent with previous reports (Fang et al. 2019; Fang et al. 2020), multiple linear regression analyses revealed that, taken together, Reasoning, Short-Term Memory and Verbal abilities significantly accounted for variability in spindle amplitude ($F(5,22) = 3.35$, $R^2 = 0.43$, $p = 0.021$). This effect was not observed for duration ($F(5,22) = 0.35$, $R^2 = 0.07$, $p = 0.867$) or density ($F(5,22) = 1.43$, $R^2 = 0.25$, $p = 0.252$). Inspection of the partial coefficients revealed that only Reasoning (controlling for Short-Term Memory and Verbal abilities) significantly, and uniquely accounted for variability in spindle amplitude ($t(22) = 2.28$, $r = 0.44$, $p = 0.033$).

When considering coupled spindles and isolated spindles separately, multiple linear regression analyses revealed that, taken together, Reasoning, Short-Term Memory and Verbal abilities accounted for variability in coupled spindle duration ($F(5,22) = 2.66$, $R^2 = 0.38$, $p = 0.050$), but not coupled spindle amplitude ($F(5,22) = 1.54$, $R^2 = 0.26$, $p = 0.217$), or density ($F(5,22) = 1.16$, $R^2 = 0.21$, $p = 0.361$). Further inspection of the partial coefficients revealed that Reasoning (controlling for Short-Term Memory and Verbal abilities) did not account for variability in coupled spindle duration ($t(22) = 1.25$, $r = 0.003$, $p = 0.224$).

Reasoning, Short-Term Memory and Verbal abilities did not account for variability in uncoupled spindle amplitude ($F(5,22) = 8.21$, $R^2 = 0.16$, $p = 0.550$), duration ($F(5,22) = 1.57$, $R^2 = 0.26$, $p = 0.210$) nor density ($F(5,22) = 1.47$, $R^2 = 0.25$, $p = 0.240$).

Cerebral activation associated with Reasoning abilities

Activation of the putamen during SW-SP coupling was positively associated with Reasoning abilities (*sr = 0.42, p = 0.039;* **Figure 3A***).* This association was not observed for uncoupled spindles (*sr = -0.03, p = 0.885)* or uncoupled slow waves (*sr = 0.31, p = 0.128).* Similarly, activation of the thalamus during SW-SP coupling was correlated with Reasoning abilities *(sr = 0.41, p = 0.042;* **Figure 3B***),* which was not observed for uncoupled spindles *(sr = 0.21, p = 0.313)* or uncoupled slow waves *(sr = 0.28, p = 0.172).* A negative correlation was observed between Reasoning abilities and hippocampal activation in response uncoupled slow waves *(sr = -0.41, p = 0.040;* **Figure 3C**). This association was not observed

for SW-SP coupling *(sr = -0.20, p = 0.333),* or uncoupled spindles *(sr = 0.09, p = 0.685)* Finally, Reasoning abilities were negatively associated with PFC activation in response to uncoupled spindles *(sr = -0.54, p = 0.005;* **Figure 3D***)*. No such association was found for SW-SP coupling *(sr = 0.05, p = 0.822)* or uncoupled slow waves *(sr = 0.03, p = 0.873)*. No significant associations were observed between Reasoning abilities and cerebral activation in any other ROIs.

Follow-up comparisons between coupled SW-SP events *vs*. uncoupled events showed that the association between activation of the putamen with Reasoning abilities during SW-SP coupled events was significantly greater than during uncoupled spindles (*z= -1.92, p = 0.027;* ***Supplemental Table S1***). The negative association with Reasoning in the hippocampus during uncoupled slow waves events was different stronger than coupled SW-SP events *(z = 3.11, p = 0.001;* ***Supplemental Table S3****)*. Additional direct comparisons between partial correlation coefficients are reported in **Supplementary Table S1-Table S7.**

Figure 3 insert

Cerebral activation associated with Verbal abilities

Significant associations were found between Verbal abilities and brain activations in frontal regions. Specifically, activation of the ACC, MCC and PFC in response to SW-SP coupling was negatively correlated with Verbal abilities (*sr = -0.50, p = 0.011; sr = -0.42, p = 0.036; sr = -0.47, p = 0.019*), which was not observed for uncoupled slow waves (*sr* =-0.28, p = 0.174; *sr =-0.13, p = 0.531;*

412 *sr =-0.05, p = 0.809*), or uncoupled spindles (*sr =0.31, p = 0.139; sr* =0.18, p = 0.388), but were positively
413 correlated with the PFC in response to uncoupled spindles (*sr =0.423, p = 0.035*). Finally, negative
414 associations were observed between the Verbal abilities and MFG activation to SW-SP coupled events
415 (*sr =-0.40, p = 0.046*) and uncoupled slow waves (*sr =-0.56, p = 0.003*), but not for uncoupled spindles
416 (*sr =0.05, p = 0.818*).

417 Follow-up comparisons between coupled SW-SP events *vs*. uncoupled events showed that the
418 association between activation of the PFC with Verbal abilities during uncoupled spindles was
419 significantly greater than during coupled SW-SP events (*z = 3.56, p < 0.001; **Supplemental Table S4***).
420 Additional direct comparisons between partial correlation coefficients for other related frontal areas are
421 reported in **Supplementary Table S1-Table S7.**

422 *Cerebral activation associated with Short-Term Memory abilities*

423 A significant negative association was found between STM scores and MFG activation in
424 response to uncoupled spindles (*sr = -0.41, p =0.042*). No such association was found for SW-SP
425 coupled events (*sr = 0.18, p =0.390*) or uncoupled slow waves (*sr = 0.28, p =0.180)*.

426 Follow-up comparisons between coupled SW-SP events *vs*. uncoupled events showed that the
427 association between activation of the MFG with STM abilities during uncoupled spindles was
428 significantly greater than during coupled SW-SP events (*z = 2.65, p = 0.004; **Supplementary Table S7**)*.

429 **Discussion**

In the present study, we investigated the functional significance of brain activation recruited during SW-coupled spindles, uncoupled spindles, and uncoupled slow waves. Converging evidence has demonstrated that spindles are one of the only, and most robust physiological indices/markers of human intelligence; in particular for Fluid Intelligence and related abilities (Fogel and Smith 2011; Fang et al. 2019; Smith et al. 2020). Most recently, simultaneous EEG-fMRI sleep studies have enabled the identification of the neural substrates and localization of the functional brain communication which support this relationship (Fang et al. 2019; Fang et al. 2021). In addition, we identified the unique cerebral activations specific to SW-SP coupling (Baena et al. 2022). However, no study to date has specifically examined the functional significance of the spontaneous cerebral activations specific to SW-SP coupling for human cognition. The results of this study revealed that when accounting for the coupling status of spindles and slow waves, the brain areas associated with stable, trait-like cognitive abilities differs, namely: 1) coupled SW-SP events recruited subcortical areas, which were positively correlated with Reasoning abilities, 2) uncoupled spindles recruited cortical frontal areas, which showed a negative correlation with Reasoning abilities, 3) uncoupled slow waves recruited the hippocampus, the extent to which was also negatively correlated with Reasoning abilities. Furthermore, in addition to Reasoning, 4) we also found mainly negative associations between Verbal abilities in frontal regions for both SW-coupled and uncoupled spindles. Taken together, these results support the view that the co-occurrence of spindles and slow waves is a functionally dissociable event from spindles on their own

448 (or, irrespective of slow wave coupling), and clarify that SW-SP coupling appears to be a key element
449 in the recruitment of cerebral substrates that support the previously identified relationship between
450 Reasoning abilities and sleep spindles.

451 Activation of the putamen was observed exclusively time-locked to SW-coupled spindles and
452 was positively correlated with Reasoning abilities. A similar pattern was observed for the thalamus.
453 Previous studies that did not consider spindle-slow wave coupling (Fang et al. 2019; Fang et al. 2020)
454 also observed a relationship between activation of these brain areas and Reasoning abilities. The
455 current study advances our understanding of this relationship, suggesting that spindle-slow wave
456 coupling is responsible for this association. Thus, suggesting that spindles in isolation may not be as
457 important as coupled events as a marker of human intellectual ability. Reasoning abilities require the
458 use of existing knowledge and experience to solve novel problems. Presumably, this requires
459 communication between subcortical areas where the new problem to solve is initially processed (van
460 den Berg et al. 2019; Berg et al. 2022) and cortical areas where existing knowledge resides (Prado et
461 al. 2011). According to the active systems consolidation hypothesis, SW-spindle complexes are an index
462 of the dialogue between subcortical and cortical regions (Born and Wilhelm 2012). Thus, the relationship
463 between SW-coupled spindles and Reasoning abilities may reflect the extent of the recruitment of
464 subcortical areas related to cognitive abilities, specifically during periods of enhanced subcortical-
465 cortical dialogue.

A different pattern of brain activation was observed for the relationship between cognitive abilities and uncoupled events. We observed hippocampal activation time-locked to uncoupled slow waves, which was negatively correlated with Reasoning abilities; this relationship was significantly stronger for uncoupled slow waves as directly compared to coupled SW-SP events. Interestingly, while the hippocampus is active during coupled SW-spindle events (Baena et al. 2022), we did not observe any relationship with Reasoning abilities. This negative association is surprising as the hippocampus plays an important role in cognitive functions like learning, spatial navigation, or memory (Muzzio et al. 2009; O'Shea et al. 2016). However, there is ongoing debate about whether the hippocampus plays a persistent role in mnemonic function, or whether its action is more crucial during the initial acquisition of new knowledge (Klinzing et al. 2019). Thus, in the absence of new information to process, this negative relationship may reflect a refractory process, but could turn positive if the night was preceded by a heavily hippocampal-dependent cognitive task. Indeed, the hippocampus has been shown to be increased during and soon after acquiring novel motor sequences and novel cognitive strategies required for problem solving (Gheysen et al. 2010; Albouy et al. 2013), as well as declarative learning (Eichenbaum 2004), and that with the passage of time, and especially an interval of sleep, in particular, the recruitment of the hippocampus is reduced (Fogel et al. 2014; Jegou et al. 2019; van den Berg et al. 2022).

Finally, mainly negative associations were observed between Verbal abilities in frontal regions for SW-coupled while positive associations were observed for uncoupled spindles, which were generally stronger associations for coupled SW-SP events *vs*. uncoupled events. Verbal IQ reflects the ability to use and remember facts, figures, events, and places; *i.e.*, the use of previous, "*crystallized*" knowledge. Our results suggest that coupled SW-SP complexes reflect the ability to utilize acquired skills or knowledge. This interpretation is line with the active system consolidation hypothesis, whereby acquired knowledge or skills are dependent on cortical brain regions (Klinzing et al. 2019).

There are several limitations worth mentioning in the present study. It was not possible to subdivide spindles into slow spindles and fast spindles nor was it possible to subdivide spindles from NREM2 and SWS due to the limited sleep duration and number of events recorded while participants were sleeping in the MRI scanner. This challenge is inherent in all EEG-fMRI sleep studies. However, there is no evidence to suggest that this would bias our results, as we have replicated and extended upon previous results that looked at full bandwidth spindles (Fang et al. 2019). In addition, we did not directly investigate any relationship between spindles, slow waves and SW-coupled spindles following new learning; this would be important to disentangle the processes involved in the night-to-night changes in brain activity that support memory consolidation, as compared to more trait-like interindividual differences in intellectual abilities.

In summary, we investigated the functional significance of brain areas recruited during SW-coupled spindles, uncoupled spindles, and uncoupled slow waves. The results of this study demonstrate that subcortical areas (*i.e.*, the putamen and the thalamus) recruited during coupled SW-SP events were the only ones positively correlated with Reasoning abilities. For the first time, we provide direct evidence that the relationship between Reasoning abilities and sleep spindles depends on spindle coupling status. In addition, the negative association between cognitive abilities and hippocampal activation time-locked to uncoupled SWs might indicate a refractory mechanism in the absence of new, intensive hippocampal-dependent memory processing. Future studies linking coupling-driven activation with consolidation of recent memories are needed to further elucidate the dissociable contribution of isolated spindles, isolated slow waves and SW-SP complexes.

Funding

This research was funded by a Canada Excellence Research Chair Grant (#215063 to A.M.O); The Natural Sciences and Engineering Research Council (NSERC) Discovery grant (RGPIN/2017–04328 to S.F.); Ministry of Research and Innovation Early Researcher Award (ERA; ER17–13-023 to S.F.).

Acknowledgments

Reprint requests should be sent to Stuart M. Fogel, Institute for Mental Health Research, University of Ottawa, Ottawa, ON, Canada, or via e-mail: sfogel@uottawa.ca.

References

Albouy G, Fogel SM, King BR, Laventure S, Benali H, Karni A, Carrier J, Robertson EM, Doyon J. 2015. Maintaining vs. enhancing motor sequence memories: Respective roles of striatal and hippocampal systems. NeuroImage. 108:423–434. doi:10.1016/j.neuroimage.2014.12.049.

Albouy G, King BR, Maquet P, Doyon J. 2013. Hippocampus and striatum: Dynamics and interaction during acquisition and sleep-related motor sequence memory consolidation. Hippocampus. 23(11):985–1004. doi:10.1002/hipo.22183.

Allen PJ, Josephs O, Turner R. 2000. A method for removing imaging artifact from continuous EEG recorded during functional MRI. Neuroimage. 12(2):230–239. doi:10.1006/nimg.2000.0599.

Allen PJ, Polizzi G, Krakow K, Fish DR, Lemieux L. 1998. Identification of EEG events in the MR scanner: the problem of pulse artifact and a method for its subtraction. NeuroImage. 8(3):229–239. doi:10.1006/nimg.1998.0361.

Andrade KC, Spoormaker VI, Dresler M, Wehrle R, Holsboer F, Sämann PG, Czisch M. 2011. Behavioral/Systems/Cognitive Sleep Spindles and Hippocampal Functional Connectivity in Human NREM Sleep. J Neurosci. 31(28):10331–10339. doi:10.1523/JNEUROSCI.5660-10.2011.

Baddeley AD. 1968. A 3 min reasoning test based on grammatical transformation. Psychon Sci. 10(10):341–342.

Baena D, Fang Z, Gibbings A, Smith D, Ray L, Doyon J, Owen AM, Fogel SM. 2022. Cerebral activation differences between slow wave-coupled and uncoupled spindles. OHBM 2022 Annual Meeting, Glasgow.

Beck AT, Epstein N, Brown G, Steer RA. 1988. An inventory for measuring clinical anxiety: psychometric properties. J Consult Clin Psychol. 56(6):893–897. doi:10.1037//0022-006x.56.6.893.

Beck AT, Steer RA, Carbin MG. 1988. Psychometric properties of the Beck Depression Inventory: Twenty-five years of evaluation. Clin Psychol Rev. 8(1):77–100. doi:10.1016/0272-7358(88)90050-5.

543 Berens P. 2009. CircStat: A MATLAB Toolbox for Circular Statistics. J Stat Softw. 31(10):1–21.
544 doi:10.18637/JSS.V031.I10.

545 Berg van den, Al-Kuwatli J, Paulin J, Ray LB, Owen AM, Fogel SM. 2019. Sleep preferentially
546 enhances memory for a cognitive strategy but not the implicit motor skills used to acquire it. Neurobiol
547 Learn Mem. 161:135–142. doi:10.1016/j.nlm.2019.04.005.

548 Berg van den, Pozzobon A, Fang Z, Al-Kuwatli J, Toor B, Ray LB, Fogel SM. 2022. Sleep Enhances
549 Consolidation of Memory Traces for Complex Problem-Solving Skills. Cereb Cortex. 32(4):653–667.
550 doi:10.1093/CERCOR/BHAB216.

551 Bergmann TO, Born J. 2018. Phase-amplitude coupling: A general mechanism for memory processing
552 and synaptic plasticity? Neuron. 97(1):10–13. doi:10.1016/J.NEURON.2017.12.023.

553 Bersagliere A, Achermann P. 2010. Slow oscillations in human non-rapid eye movement sleep
554 electroencephalogram: effects of increased sleep pressure. J Sleep Res. 19(1p2):228–237.
555 doi:10.1111/j.1365-2869.2009.00775.x.

556 Bódizs R, Kis T, Lázár AS, Havrán L, Rigó P, Clemens Z, Halász P. 2005. Prediction of general
557 mental ability based on neural oscillation measures of sleep. J Sleep Res. 14(3):285–292.
558 doi:10.1111/j.1365-2869.2005.00472.x.

559 Bódizs R, Lázár AS, Rigó P. 2008. Correlation of visuospatial memory ability with right parietal EEG
560 spindling during sleep. Acta Physiol Hung. 95(3):297–306. doi:10.1556/APhysiol.95.2008.3.5.

561 Born J, Wilhelm I. 2012. System consolidation of memory during sleep. Psychol Res. 76(2):192–203.
562 doi:10.1007/s00426-011-0335-6.

563 Branger P, Arenaza-Urquijo EM, Tomadesso C, Mézenge F, André C, de Flores R, Mutlu J, de La
564 Sayette V, Eustache F, Chételat G, et al. 2016. Relationships between sleep quality and brain volume,
565 metabolism, and amyloid deposition in late adulthood. Neurobiol Aging. 41:107–114.
566 doi:10.1016/j.neurobiolaging.2016.02.009.

567 Brewer-Deluce D, Wilson TD, Owen AM. Cognitive Function in Varsity Football Athletes is Maintained
568 in the Absence of Concussion. FASEB J. 31:745.7-745.7.
569 doi:10.1096/FASEBJ.31.1_SUPPLEMENT.745.7.

570 Caporro M, Haneef Z, Yeh HJ, Lenartowicz A, Buttinelli C, Parvizi J, Stern JM. 2012. Functional MRI
571 of sleep spindles and K-complexes. Clin Neurophysiol. 123(2):303–309.
572 doi:10.1016/J.CLINPH.2011.06.018.

573 Casey BJ, Tottenham N, Liston C, Durston S. 2005. Imaging the developing brain: what have we
574 learned about cognitive development? Trends Cogn Sci. 9(3):104–110. doi:10.1016/j.tics.2005.01.011.

575 Cattell RB. 1940. A culture-free intelligence test. J Educ Psychol. 31(3):161–179.
576 doi:10.1037/h0059043.

577 Cattell RB. 1963. Theory of fluid and crystallized intelligence: A critical experiment. J Educ Psychol.
578 54(1):1–22.

579 Collins P, Roberts AC, Dias R, Everitt BJ, Robbins TW. 1998. Perseveration and Strategy in a Novel
580 Spatial Self-Ordered Sequencing Task for Nonhuman Primates: Effects of Excitotoxic Lesions and
581 Dopamine Depletions of the Prefrontal Cortex. J Cogn Neurosci. 10(3):332–354.
582 doi:10.1162/089892998562771.

583 Corsi P. 1973. Human memory and the medial temporal region of the brain. Diss Abstr Int. 34(2-
584 B):891.

585 Delorme A, Makeig S. 2004. EEGLAB: An open source toolbox for analysis of single-trial EEG
586 dynamics including independent component analysis. J Neurosci Methods. 134(1):9–21.
587 doi:10.1016/j.jneumeth.2003.10.009.

588 Douglass AB, Bornstein RF, Nino-Murcia G, Keenan S, Miles L, Zarcone VP, Guilleminault C, Dement
589 WC, Jr VPZ, Guilleminault C, et al. 1994. The Sleep Disorders Questionnaire. I: Creation and
590 multivariate structure of SDQ. Sleep. 17(2):160. doi:10.1093/sleep/17.2.160.

591 Eichenbaum H. 2004. Hippocampus: Cognitive Processes and Neural Representations that Underlie
592 Declarative Memory. Neuron. 44(1):109–120. doi:10.1016/j.neuron.2004.08.028.

593 Fang Z, Ray LBB, Owen AMM, Fogel SM. 2019. Brain Activation Time-Locked to Sleep Spindles
594 Associated With Human Cognitive Abilities. Front Neurosci. 13(FEB):46.
595 doi:10.3389/fnins.2019.00046.

596 Fang Z, Ray LBBLB, Houldin E, Smith D, Owen AMAMM, Fogel SM. 2020. Sleep Spindle-dependent
597 Functional Connectivity Correlates with Cognitive Abilities. J Cogn Neurosci. 32(3):446–466.
598 doi:10.1162/jocn_a_01488.

599 Fang Z, Sergeeva V, Ray LB, Viczko J, Owen AM, Fogel SM. 2017. Sleep spindles and intellectual
600 ability: Epiphenomenon or directly related? J Cogn Neurosci. 29(1):167–182.
601 doi:10.1162/jocn_a_01034.

602 Fang Z, Smith DM, Houldin E, Ray L, Owen AM, Fogel SM. 2021. The relationship between cognitive
603 ability and BOLD activation across sleep–wake states. Brain Imaging Behav.(0123456789).
604 doi:10.1007/s11682-021-00504-w.

605 Fogel S, Albouy G, King BR, Lungu O, Vien C, Bore A, Pinsard B, Benali H, Carrier J, Doyon J. 2017.
606 Reactivation or transformation? Motor memory consolidation associated with cerebral activation time-
607 locked to sleep spindles. PLOS ONE. 12(4):e0174755. doi:10.1371/JOURNAL.PONE.0174755.

608 Fogel S, Nader R, Cote K, Smith C. 2007. Sleep spindles and learning potential. Behav Neurosci.
609 121(1):1–10. doi:10.1037/0735-7044.121.1.1.

610 Fogel S, Smith C. 2011. The function of the sleep spindle: A physiological index of intelligence and a
611 mechanism for sleep-dependent memory consolidation. Neurosci Biobehav Rev. 35(5):1154–1165.
612 doi:10.1016/j.neubiorev.2010.12.003.

613 Fogel SM, Albouy G, King BR, Vien C, Karni A, Benali H, Maquet P, Carrier J, Doyon J. 2014. Motor
614 memory consolidation depends upon reactivation driven by the action of sleep spindles. J Sleep Res.
615 23(s1):47. doi:DOI: 10.1111/jsr.12213.

616 Fogel SM, Smith CT. 2006. Learning-dependent changes in sleep spindles and Stage 2 sleep. J Sleep
617 Res. 15(3):250–255. doi:10.1111/j.1365-2869.2006.00522.x.

618 Fogel SM, Vien C, Karni A, Benali H, Carrier J, Doyon J, Albouy G. 2017. Sleep spindles: A
619 physiological marker of age-related changes in grey matter in brain regions supporting motor skill
620 memory consolidation. Neurobiol Aging. 49:154–164. doi:10.1016/j.neurobiolaging.2016.10.009.

621 Folstein MF, Folstein SE, McHugh PR. 1975. “Mini-mental state”. A practical method for grading the
622 cognitive state of patients for the clinician. J Psychiatr Res. 12(3):189–198. doi:10.1016/0022-
623 3956(75)90026-6.

624 Friston KJ, Williams S, Howard R, Frackowiak RSJ, Turner R. 1996. Movement-Related effects in
625 fMRI time-series. Magn Reson Med. 35(3):346–355. doi:10.1002/MRM.1910350312.

626 Gaillard JM, Blois R. 1981. Spindle density in sleep of normal subjects. Sleep. 4(4):385.

627 Gennaro LD, Ferrara M, Vecchio, Curcio G, Bertini M. 2005. An electroencephalographic fingerprint of
628 human sleep. Neuroimage. 26(1):114–122. doi:S1053-8119(05)00049-2 [pii]
629 10.1016/j.neuroimage.2005.01.020.

630 Gheysen F, Opstal FV, Roggeman C, Waelvelde HV, Fias W. 2010. Hippocampal contribution to early
631 and later stages of implicit motor sequence learning. Exp Brain Res. 202(4):795–807.
632 doi:10.1007/s00221-010-2186-6.

633 Gould RL, Brown RG, Owen AM, Bullmore ET, Howard RJ. 2006. Task-induced deactivations during
634 successful paired associates learning: an effect of age but not Alzheimer's disease. NeuroImage.
635 31(2):818–31.

636 Hampshire A, Highfield RR, Parkin BL, Owen AM. 2012. Fractionating human intelligence. Neuron.
637 76(6):1225–1237. doi:10.1016/j.neuron.2012.06.022.

638 Helfrich RF, Lendner JD, Mander BA, Guillen H, Paff M, Mnatsakanyan L, Vadera S, Walker MP, Lin
639 JJ, Knight RT. 2019. Bidirectional prefrontal-hippocampal dynamics organize information transfer
640 during sleep in humans. Nat Commun. 10(1):3572. doi:10.1038/s41467-019-11444-x.

641 Helfrich RF, Mander BA, Jagust WJ, Knight RT, Walker M. 2018. Old brains come uncoupled in sleep:
642 Slow wave-spindle synchrony, brain atrophy, and forgetting. Neuron. 97(1):221–230.
643 doi:10.1016/J.NEURON.2017.11.020.

644 Iber C, Ancoli-Israel S, Chesson AL, Quan SF. 2007. The AASM manual for the scoring of sleep and
645 associated events: rules, terminology and technical specifications. 1st ed. American Academy of
646 Sleep Medicine, Westchester, IL.

647 Inoue S, Matsuzawa T. 2007. Working memory of numerals in chimpanzees. Curr Biol.
648 17(23):R1004—-R1005.

649 Jegou A, Schabus M, Gosseries O, Dahmen B, Albouy G, Desseilles M, Sterpenich V, Phillips C,
650 Maquet P, Grova C, et al. 2019. Cortical reactivations during sleep spindles following declarative
651 learning. NeuroImage. 195:104–112. doi:10.1016/j.neuroimage.2019.03.051.

652 Klinzing JG, Niethard N, Born J. 2019. Mechanisms of systems memory consolidation during sleep.
653 Nat Neurosci. 22(10):1598–1610. doi:10.1038/s41593-019-0467-3.

654 Laufs H, Walker MC, Lund TE. 2007. 'Brain activation and hypothalamic functional connectivity during
655 human non-rapid eye movement sleep: An EEG/fMRI study'-its limitations and an alternative
656 approach. Brain J Neurol. 130(7):e75–e75. doi:10.1093/brain/awm084.

657 Laventure S, Pinsard B, Lungu O, Carrier J, Fogel SM, Benali H, Lina J-MM, Boutin A, Doyon J. 2018.
658 Beyond spindles: interactions between sleep spindles and boundary frequencies during cued
659 reactivation of motor memory representations. Sleep. 41(9):1–14. doi:10.1093/sleep/zsy142.

660 Lenhard W, Lenhard A. 2014. Testing the Significance of Correlations.
661 doi:10.13140/RG.2.1.2954.1367.

662 Maingret N, Girardeau G, Todorova R, Goutierre M, Zugaro M. 2016. Hippocampo-cortical coupling
663 mediates memory consolidation during sleep. Nat Neurosci. 19(7):959–966. doi:10.1038/nn.4304.

664 Mantini D, Perrucci MG, Cugini S, Ferretti A, Romani GL, Gratta CD. 2007. Complete artifact removal
665 for EEG recorded during continuous fMRI using independent component analysis. Neuroimage.
666 34(2):598–607. doi:10.1016/j.neuroimage.2006.09.037.

667 Mölle M, Bergmann TO, Marshall L, Born J. 2011. Fast and Slow Spindles during the Sleep Slow
668 Oscillation: Disparate Coalescence and Engagement in Memory Processing. Sleep. 34(10):1411–
669 1421. doi:10.5665/SLEEP.1290.

670 Mulert C, Lemieux L. 2010. EEG-fMRI: Physiological Basis, Technique and Applications. illustrate ed.
671 Springer.

672 Mullinger KJ, Yan WX, Bowtell R. 2011. Reducing the gradient artefact in simultaneous EEG-fMRI by
673 adjusting the subject's axial position. NeuroImage. 54(3):1942–1950.
674 doi:10.1016/j.neuroimage.2010.09.079.

675 Muzzio IA, Kentros C, Kandel E. 2009. What is remembered? Role of attention on the encoding and
676 retrieval of hippocampal representations. J Physiol. 587(12):2837–2854.
677 doi:10.1113/JPHYSIOL.2009.172445.

678 Nader R, Smith C. 2009 Sep. A Role For Stage 2 Sleep in Memory Processing. Sleep Brain Plast.:87–
679 98. doi:10.1093/ACPROF:OSO/9780198574002.003.0005.

680 Ngo H. V., J F, B S, Ngo Hong Viet, Fell J, Staresina B. 2020. Sleep spindles mediate hippocampal-
681 neocortical coupling during long-duration ripples. eLife. 9:1–18. doi:10.7554/ELIFE.57011.

682 O'Shea A, Cohen RA, Porges EC, Nissim NR, Woods AJ. 2016. Cognitive aging and the hippocampus
683 in older adults. Front Aging Neurosci. 8(DEC):298. doi:10.3389/FNAGI.2016.00298/BIBTEX.

684 Prado J, Chadha A, Booth JR. 2011. The Brain Network for Deductive Reasoning: A Quantitative
685 Meta-analysis of 28 Neuroimaging Studies. J Cogn Neurosci. 23(11):3483.
686 doi:10.1162/JOCN_A_00063.

687 Ray LB, Sockeel S, Soon M, Bore A, Myhr A, Stojanoski B, Cusack R, Owen AM, Doyon J, Fogel SM.
688 2015. Expert and crowd-sourced validation of an individualized sleep spindle detection method
689 employing complex demodulation and individualized normalization. Front Hum Neurosci. 9(9).
690 doi:10.3389/fnhum.2015.00507.

691 Saletin JM, Helm E van der, Walker M. 2013. Structural brain correlates of human sleep oscillations.
692 NeuroImage. 83(C):658–668. doi:10.1016/j.neuroimage.2013.06.021.

693 Sandman CA, Head K, Muftuler LT, Su L, Buss C, Poggi E. 2014. NeuroImage Shape of the basal
694 ganglia in preadolescent children is associated with cognitive performance. NeuroImage. 99:93–102.
695 doi:10.1016/j.neuroimage.2014.05.020.

696 Schabus M, Dang-Vu TT, Albouy G, Balteau E, Boly M, Carrier J, Darsaud A, Degueldre C, Desseilles
697 M, Gais S, et al. 2007. Hemodynamic cerebral correlates of sleep spindles during human non-rapid
698 eye movement sleep. Proc Natl Acad Sci. 104(32):13164–13169. doi:10.1073/PNAS.0703084104.

699 Schabus M, Hödlmoser K, Gruber G, Sauter C, Anderer P, Klösch G, Parapatics S, Saletu B,
700 Klimesch W, Zeitlhofer J. 2006. Sleep spindle-related activity in the human EEG and its relation to
701 general cognitive and learning abilities. Eur J Neurosci. 23(7):1738–1746. doi:10.1111/j.1460-
702 9568.2006.04694.x.

703 Shallice T. 1982. Specific impairments of planning. Philos Trans R Soc Lond.:199–209.

704 Silverman I, Choi J, Mackewn A. 2000. Evolved mechanisms underlying wayfinding: Further studies
705 on the hunter-gatherer theory of spatial sex differences. Evol Hum Behav. 21(3):201–213.

706 Silverstein LD, Levy CM. 1976. The stability of the sigma sleep spindle. Electroencephalogr Clin
707 Neurophysiol. 40(6):666–670.

708 Smith D, Fang Z, Thompson K, Fogel SM. 2020. Sleep and individual differences in intellectual
709 abilities. Curr Opin Behav Sci. 33:126–131. doi:10.1016/j.cobeha.2020.02.011.

710 Srivastava G, Crottaz-Herbette S, Lau KM, Glover GH, Menon V. 2005. ICA-based procedures for
711 removing ballistocardiogram artifacts from EEG data acquired in the MRI scanner. NeuroImage.
712 24(1):50–60. doi:10.1016/j.neuroimage.2004.09.041.

713 Stroop JR. 1935. Studies of interference in serial verbal reactions. J Exp Psychol. 18(6):643–662.
714 doi:10.1037/h0054651.

715 Treisman AM, Gelade G. 1980. A feature-integration theory of attention. Cognit Psychol. 12(1):97–
716 136.

717 Tyvaert L, LeVan P, Grova C, Dubeau F, Gotman J. 2008. Effects of fluctuating physiological rhythms
718 during prolonged EEG-fMRI studies. Clin Neurophysiol. 119(12):2762–2774.
719 doi:10.1016/j.clinph.2008.07.284.

720 Ujma, Konrad, Genzel, Bleifuss, Simor, Pótári A, Körmendi J, Gombos F, Steiger A, Bódizs R, et al.
721 2014. Sleep spindles and intelligence: Evidence for a sexual dimorphism. J Neurosci. 34(49):16358–
722 16368. doi:10.1523/JNEUROSCI.1857-14.2014.

723 Ujma PP, Bódizs R, Gombos F, Stintzing J, Konrad BN, Genzel L, Steiger A, Dresler M. 2015. Nap
724 sleep spindle correlates of intelligence. Sci Rep. 5:17159. doi:10.1038/srep17159.

725 Wechsler DA. 1981. Wechsler Adult Intelligence Scale–Revised. N Y Psychol Corp.

726 Wild CJ, Nichols ES, Battista ME, Stojanoski B, Owen AM. 2018. Dissociable effects of self-reported
727 daily sleep duration on high-level cognitive abilities. Sleep. 41(12). doi:10.1093/sleep/zsy182.

728

Table 1. Descriptive statistics of the three CBS subscales (Reasoning, STM, and Verbal abilities).

IQ measures	**Range**	**Mean ± SD**	**Median**
Reasoning	78.84-108.17	95.51 ± 7.30	96.40
STM	84.38-115.33	101.65 ± 6.88	102.40
Verbal	88.51-110.92	99.60 ± 5.20	99.52

729
730
731
732

Table 2. Sleep architecture during EEG–fMRI recording session.

	N	*M*	*SD*
Wake (min)	25	26.60	20.60
NREM1 (min)	25	5.63	4.34
NREM2 (min)	28	24.32	14.56
SWS (min)	20	14.77	17.17
NREM (min)	28	39.90	19.40
REM (min)	8	17.80	10.76
Total sleep (min)	28	44.98	23.90
Sleep latency (min)	28	7.71	10.00

NREM = non-rapid eye movement; SWS = slow wave sleep; REM = rapid eye movement.

733
734
735
736

Table 3. Sleep spindle parameters for coupled SW-SP and uncoupled spindles during NREM sleep from EEG–fMRI recording sessions.

	Coupled SW-SP		**Uncoupled spindles**			
	M	**SEM**	**M**	**SEM**	**T-statistic**	**P-value**
Number	215.64	45.90	264.43	76.23	-0.56	0.580
Duration (s)	0.70	0.02	0.70	0.02	-0.16	0.870
Amplitude (uV)	34.43	1.82	29.10	1.63	3.61	0.001
Density	3.92	0.65	4.74	1.00	-0.66	0.510

M = mean; SEM = standard error of the mean. *P*-values for paired samples t-test between spindle parameters.

737
738

Figure 1. Study Design. Participants underwent an initial screening to rule out any signs of sleep disorders, unusual sleep habits, or other health-related criteria and MRI compatibility. Eligible participants then visited the sleep laboratory for the orientation session at least one week before the EEG-fMRI sleep recording night, in which participants were given detailed instructions about the study procedure, the sleep diary, and an activity monitor. Participants completed the CBS tests online and kept a regular sleep-wake cycle for at least 1 week prior to the sleep recording. Compliance with this schedule was assessed using both sleep diaries and wrist actigraphy. Finally, participants completed the EEG-fMRI sleep recording session beginning at 21:00 h, with lights out for the sleep session at 22:00 h. The sleep session ended by midnight (24:00 h).

Figure 2. **A:** Coupled slow wave – spindle histogram for all participants. Each bar represents the number of coupled spindles detected in an interval of 200 ms divided by the total number of spindles. Average slow wave osciallation for all participants is superimposed In black. **B:** Circular plot of preferred phase for each individual (slow wave phase at spindle amplitude maximum). Grey dots denote an individual preferred phase (0^o slow wave down-to-up state, $\pm 180^o$ slow wave up-to-down state). The direction of the line indicates the preferred direction of the grand average. Most individuals exhibit spindles adjacent to, or immediately following the positive slow wave peak at 0^o.

Figure 3. Associations between Reasoning abilities and cerebral activation in (A) bilateral putamen; (B) bilateral thalamus; (C) bilateral hippocampus; (D) prefrontal cortex (PFC).

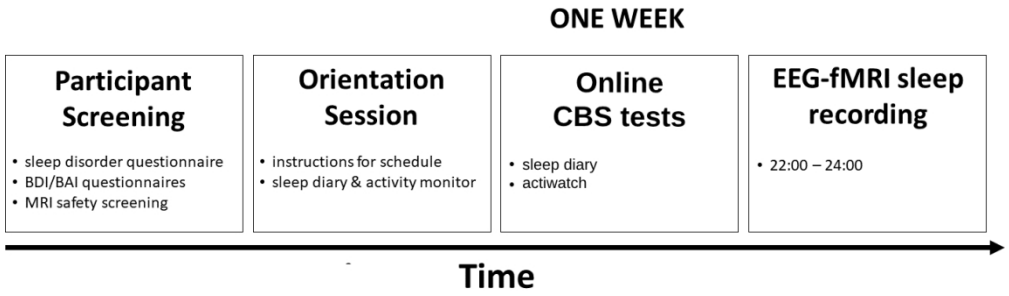

Figure 1. Study Design. Participants underwent an initial screening to rule out any signs of sleep disorders, unusual sleep habits, or other health-related criteria and MRI compatibility. Eligible participants then visited the sleep laboratory for the orientation session at least one week before the EEG-fMRI sleep recording night, in which participants were given detailed instructions about the study procedure, the sleep diary, and an activity monitor. Participants completed the CBS tests online and kept a regular sleep-wake cycle for at least 1 week prior to the sleep recording. Compliance with this schedule was assessed using both sleep diaries and wrist actigraphy. Finally, participants completed the EEG-fMRI sleep recording session beginning at 21:00 h, with lights out for the sleep session at 22:00 h. The sleep session ended by midnight (24:00 h).

375x128mm (96 x 96 DPI)

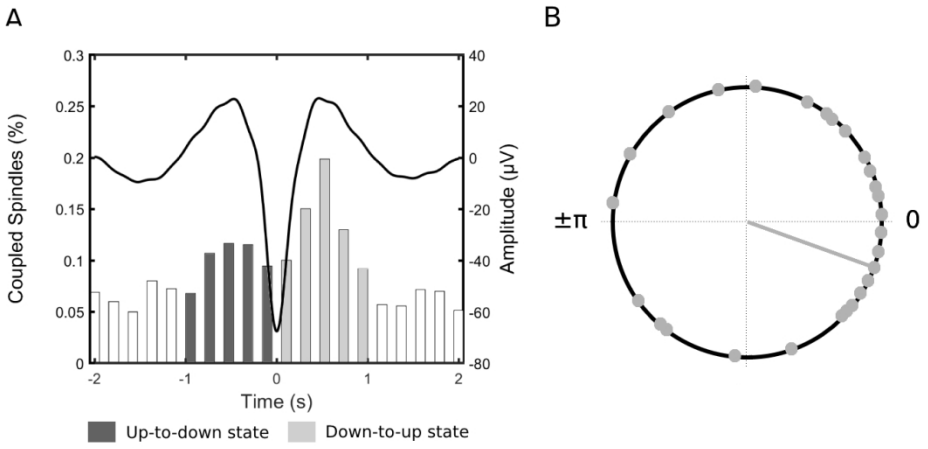

Figure 2. A: Coupled slow wave – spindle histogram for all participants. Each bar represents the number of coupled spindles detected in an interval of 200 ms divided by the total number of spindles. Average slow wave osciallation for all participants is superimposed In black. B: Circular plot of preferred phase for each individual (slow wave phase at spindle amplitude maximum). Grey dots denote an individual preferred phase (0o slow wave down-to-up state, ±180o slow wave up-to-down state). The direction of the line indicates the preferred direction of the grand average. Most individuals exhibit spindles adjacent to, or immediately following the positive slow wave peak at 0o.

383x198mm (96 x 96 DPI)

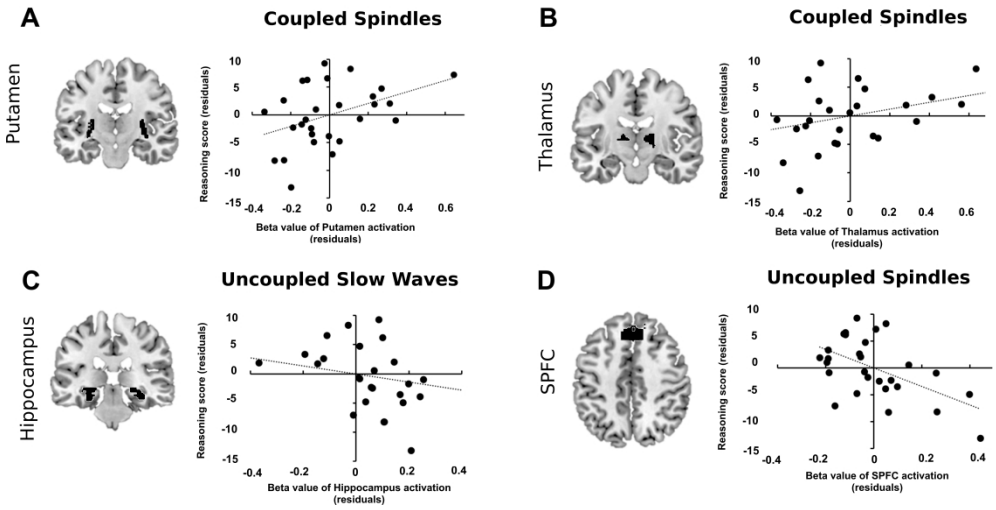

Figure 3. Associations between Reasoning abilities and cerebral activation in (A) bilateral putamen; (B) bilateral thalamus; (C) bilateral hippocampus; (D) prefrontal cortex (PFC).

694x351mm (300 x 300 DPI)

738 **Supplemental Tables**
739

Table S1. Regression: Putamen activation & cognitive abilities

Overall regression effects				
Region	**Event type**	**F (4, 23)**	**R^2**	**p-value**
Putamen	Coupled SW-SP	2.49	0.30	0.072
	Uncoupled spindle	0.08	0.01	0.987
	Uncoupled slow wave	1.13	0.16	0.369
Partial coefficients				
Subtest	**Event type**	**t (23)**	**partial r**	**p-value**
Reasoning	Coupled SW-SP	2.19	0.42	0.039*
	Uncoupled spindle	-0.15	-0.03	0.885
	Uncoupled slow wave	1.58	0.31	0.128
Verbal	Coupled SW-SP	-0.03	-0.01	0.978
	Uncoupled spindle	0.28	0.06	0.781
	Uncoupled slow wave	-1.58	-0.31	0.128
STM	Coupled SW-SP	-1.15	-0.23	0.262
	Uncoupled spindle	0.34	0.07	0.737
	Uncoupled slow wave	1.02	0.21	0.317
Follow-up comparisons of partial correlation coefficients				
Subtest	**Event type 1**	**Event type 2**	**z**	**p-value**
Reasoning	Coupled SW-SP	Uncoupled spindle	-1.92	0.027*
	Coupled SW-SP	Uncoupled slow wave	1.29	0.099

740

741

Table S2. Regression: Thalamus activation & cognitive abilities

Overall regression effects				
Region	**Event type**	**F (4, 23)**	**R^2**	**p-value**
Thalamus	Coupled SW-SP	1.28	0.18	0.305
	Uncoupled spindle	1.38	0.19	0.274
	Uncoupled slow wave	0.72	0.11	0.586
Partial coefficients				
Subtest	**Event type**	**t (23)**	**partial r**	**p-value**
Reasoning	Coupled SW-SP	2.15	0.41	0.042*
	Uncoupled spindle	1.03	0.21	0.313
	Uncoupled slow wave	1.41	0.28	0.172
Verbal	Coupled SW-SP	-1.49	-0.30	0.149
	Uncoupled spindle	-0.28	-0.06	0.785
	Uncoupled slow wave	-0.68	-0.14	0.506
STM	Coupled SW-SP	-0.38	-0.08	0.709
	Uncoupled spindle	0.54	0.11	0.598
	Uncoupled slow wave	0.23	0.05	0.818
Follow-up comparisons of partial correlation coefficients				
Subtest	**Event type 1**	**Event type 2**	**z**	**p-value**
Reasoning	Coupled SW-SP	Uncoupled spindle	-1.03	0.151
	Coupled SW-SP	Uncoupled slow wave	2.39	0.008*

742

743

Table S3. Regression: Hippocampus activation & cognitive abilities

Overall regression effects				
Region	**Event type**	**F (4, 23)**	**R^2**	**p-value**
Hippocampus	Coupled spindle	2.31	0.29	0.089
	Uncoupled spindle	1.19	0.17	0.340
	Uncoupled slow wave	1.23	0.18	0.327
Partial coefficients				
Subtest	**Event type**	**t (23)**	**partial r**	**p-value**
Reasoning	Coupled SW-SP	-0.99	-0.20	0.333
	Uncoupled spindle	0.41	0.09	0.685
	Uncoupled slow wave	-2.18	-0.41	0.040*
Verbal	Coupled SW-SP	1.90	0.37	0.070
	Uncoupled spindle	-0.06	-0.01	0.955
	Uncoupled slow wave	1.40	0.28	0.174
STM	Coupled SW-SP	0.19	0.04	0.854
	Uncoupled spindle	1.62	0.32	0.120
	Uncoupled slow wave	-0.08	-0.02	0.939
Follow-up comparisons of partial correlation coefficients				
Subtest	**Event type 1**	**Event type 2**	**z**	**p-value**
Reasoning	Coupled SW-SP	Uncoupled slow wave	3.11	0.001*

744

745

Table S4. Regression: PFC activation & cognitive abilities

Overall regression effects				
Region	**Event type**	**F (4, 23)**	**R^2**	**p-value**
SPFC	Coupled SW-SP	2.35	0.29	0.084
	Uncoupled spindle	3.69	0.39	0.018*
	Uncoupled slow wave	0.13	0.02	0.970
Partial coefficients				
Subtest	**Event type**	**t (23)**	**partial r**	**p-value**
Reasoning	Coupled SW-SP	0.23	0.05	0.822
	Uncoupled spindle	-3.09	-0.54	0.005*
	Uncoupled slow wave	0.16	0.03	0.873
Verbal	Coupled SW-SP	-2.53	-0.47	0.019*
	Uncoupled spindle	2.24	0.42	0.035*
	Uncoupled slow wave	-0.25	-0.05	0.809
STM	Coupled SW-SP	0.77	0.16	0.451
	Uncoupled spindle	1.43	0.29	0.167
	Uncoupled slow wave	-0.46	-0.10	0.648
Follow-up comparisons of partial correlation coefficients				
Subtest	**Event type 1**	**Event type 2**	**z**	**p-value**
Reasoning	Coupled SW-SP	Uncoupled spindle	-1.82	0.035*
Verbal	Coupled SW-SP	Uncoupled spindle	1.87	0.030*
	Coupled SW-SP	Uncoupled slow wave	3.56	>0.001*

746

Table S5. Regression: ACC activation & cognitive abilities

Overall regression effects				
Region	**Event type**	**F (4, 23)**	**R^2**	**p-value**
ACC	Coupled SW-SP	2.48	0.30	0.072
	Uncoupled spindle	3.07	0.35	0.036*
	Uncoupled slow wave	1.26	0.18	0.314
Partial coefficients				
Subtest	**Event type**	**t (23)**	**partial r**	**p-value**
Reasoning	Coupled SW-SP	0.99	0.20	0.335
	Uncoupled spindle	0.34	0.07	0.739
	Uncoupled slow wave	-0.15	-0.03	0.884
Verbal	Coupled SW-SP	-2.78	-0.50	0.011*
	Uncoupled spindle	1.54	0.31	0.139
	Uncoupled slow wave	-1.40	-0.28	0.174
STM	Coupled SW-SP	0.37	0.08	0.714
	Uncoupled spindle	0.40	0.08	0.690
	Uncoupled slow wave	-0.32	-0.07	0.750
Follow-up comparisons of partial correlation coefficients				
Subtest	**Event type 1**	**Event type 2**	**z**	**p-value**
Verbal	Coupled SW-SP	Uncoupled spindle	0.56	0.287
	Coupled SW-SP	Uncoupled slow wave	5.07	>0.001*

747

748

Table S6. Regression: MCC activation & cognitive abilities

Overall regression effects				
Region	**Event type**	**F (4, 23)**	**R^2**	**p-value**
MCC	Coupled SW-SP	1.28	0.18	0.308
	Uncoupled spindle	0.99	0.15	0.435
	Uncoupled slow wave	0.96	0.14	0.450
Partial coefficients				
Subtest	**Event type**	**t (23)**	**partial r**	**p-value**
Reasoning	Coupled SW-SP	1.345	0.27	0.192
	Uncoupled spindle	0.58	0.12	0.567
	Uncoupled slow wave	-0.42	-0.09	0.677
Verbal	Coupled SW-SP	-2.22	-0.42	0.036*
	Uncoupled spindle	0.88	0.18	0.388
	Uncoupled slow wave	-0.64	-0.13	0.531
STM	Coupled SW-SP	0.93	0.19	0.363
	Uncoupled spindle	-1.82	-0.35	0.082
	Uncoupled slow wave	0.69	0.14	0.496
Follow-up comparisons of partial correlation coefficients				
Subtest	**Event type 1**	**Event type 2**	**z**	**p-value**
Verbal	Coupled SW-SP	Uncoupled spindle	1.54	0.062
	Coupled SW-SP	Uncoupled slow wave	3.39	>0.001*

749

Table S7. Regression: MFG activation & cognitive abilities

Overall regression effects				
Region	**Event type**	**F (4, 23)**	**R^2**	**p-value**
MFG	Coupled SW-SP	1.53	0.21	0.226
	Uncoupled spindle	1.34	0.19	0.285
	Uncoupled slow wave	4.66	0.45	0.007*
Partial coefficients				
Subtest	**Event type**	**t (23)**	**partial r**	**p-value**
Reasoning	Coupled SW-SP	0.47	0.10	0.643
	Uncoupled spindle	0.23	0.05	0.822
	Uncoupled slow wave	-0.27	-0.06	0.788
Verbal	Coupled SW-SP	-2.11	-0.40	0.046*
	Uncoupled spindle	0.23	0.05	0.818
	Uncoupled slow wave	-3.26	-0.56	0.003*
STM	Coupled SW-SP	0.88	0.18	0.390
	Uncoupled spindle	-2.15	-0.41	0.042*
	Uncoupled slow wave	1.38	0.28	0.180
Follow-up comparisons of partial correlation coefficients				
Subtest	**Event type 1**	**Event type 2**	**z**	**p-value**
Verbal	Coupled SW-SP	Uncoupled spindle	2.43	0.007*
	Coupled SW-SP	Uncoupled slow wave	3.79	>0.001*
STM	Coupled SW-SP	Uncoupled spindle	2.65	0.004*